GW in Magnetism: where it succeeds, where not

Mark van Schilfgaarde, King's College London

LDA description of Ni, Fermi liquid regime

Classic ARPES study: Himpsel, Knapp, Eastman PRB 19, 2919

Exchange splitting:

$\Delta E_x = L_{3\downarrow} - L_{3\uparrow} \approx 0.3$ eV

0.6 eV in LDA

s band wrongly placed

Poor dispersion in Λ_1 band

LDA predicts M=0.6 μ_B, close to expt. But … good agreement is fortuitous …

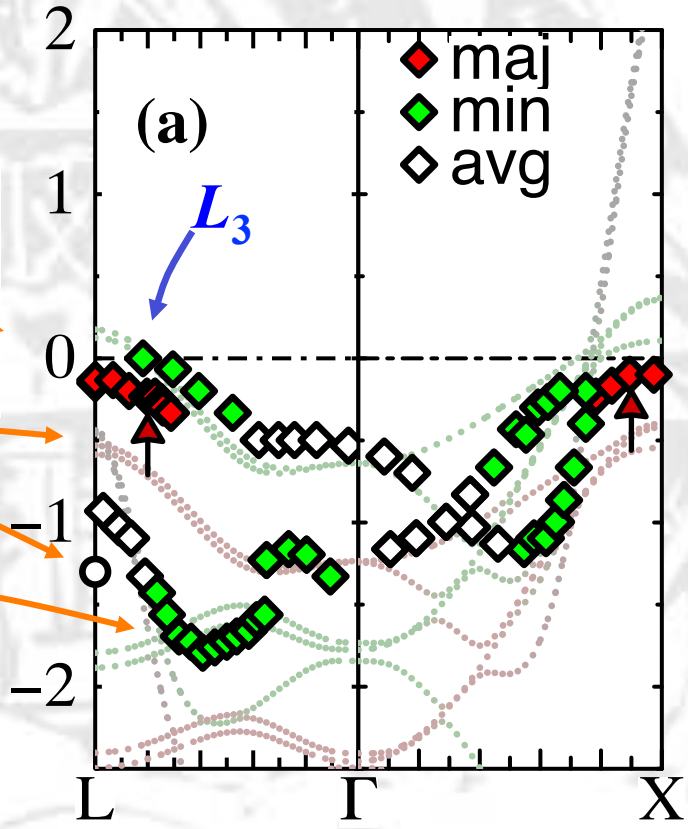

Properties of the GW Approximation

Hartree Fock

$$\Sigma_x = i\int G(\mathbf{r},\mathbf{r}')\frac{1}{|\mathbf{r}-\mathbf{r}'|}d^3\mathbf{r}' = iGv$$

GW

$$\frac{1}{|\mathbf{r}-\mathbf{r}'|} \to \varepsilon^{-1}v = W; \quad \Sigma = iGW$$

✔ ω-dependent W and Σ – outside one-electron picture.

✔ Nonlocal W and Σ --- very important.

✔ Van der Waals interactions lie within the theory

✔ "exact" in the limit of weak correlations.

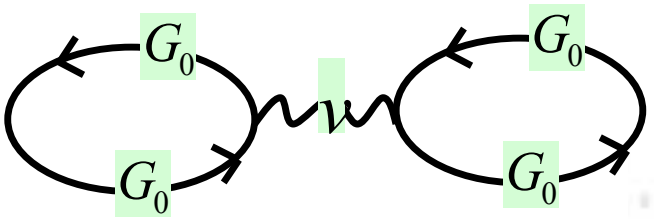

✘ W screens v in the charge channel only … its dynamical fluctuations are plasmons.
Σ knows about spin because through the Fock exchange no fluctuations in the spin channel.

✘ Other interactions (particle-particle) are missing

GW Approximation and self-consistency

Neglect vertex … vastly simpler

$$P(1,2) = -iGG, \quad \Sigma = iGW$$

G and Σ are usually generated from some effective noninteracting one-body hamiltonian H_0, usu. $H_0 = H_{\mathrm{LDA}}$

$$(h + V_H + V_x)\psi_s = \varepsilon_s \psi_s$$

$$G = \sum_s \frac{\psi_s \psi_s^*}{\omega - \varepsilon_s \pm i\delta}$$

Often problematic …

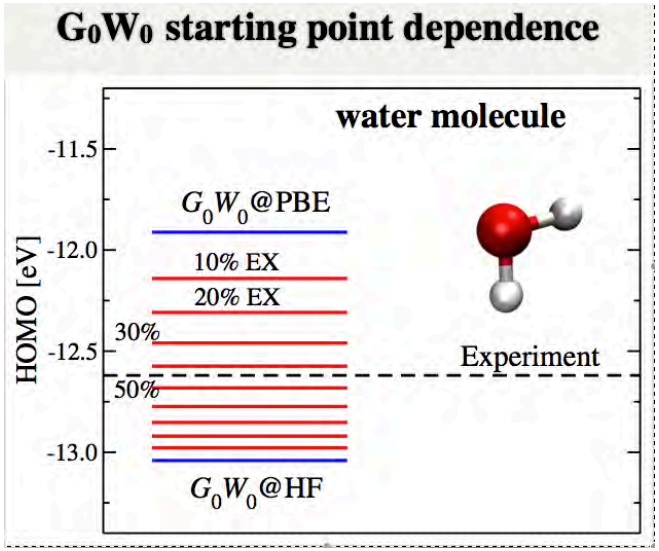

Patrick Rinke, CECAM (Toulouse, 2013)

Severe errors

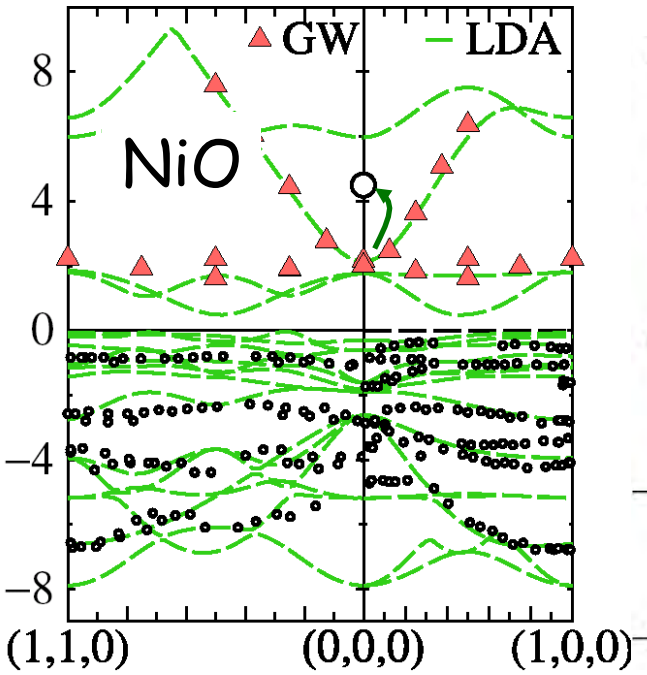

Nonsensical FS

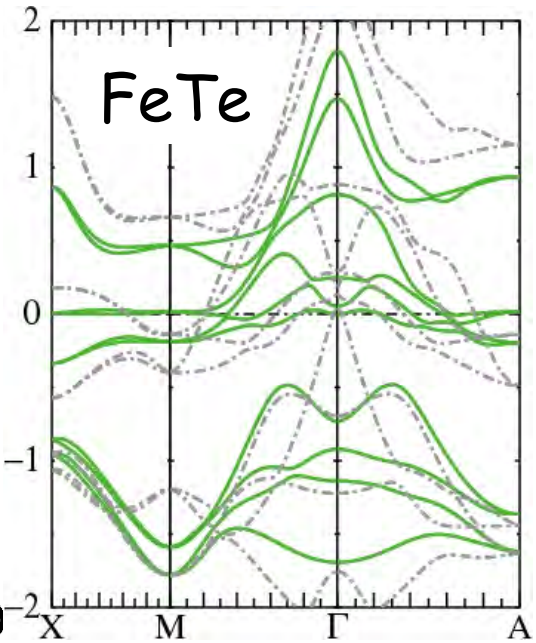

Problems with self-consistency

Iterate G to self-consistency:

GW is problematic even for the homogeneous gas

$$G_0 \rightarrow \Sigma \rightarrow$$
$$G \rightarrow \Sigma \rightarrow G \rightarrow \Sigma \ldots$$

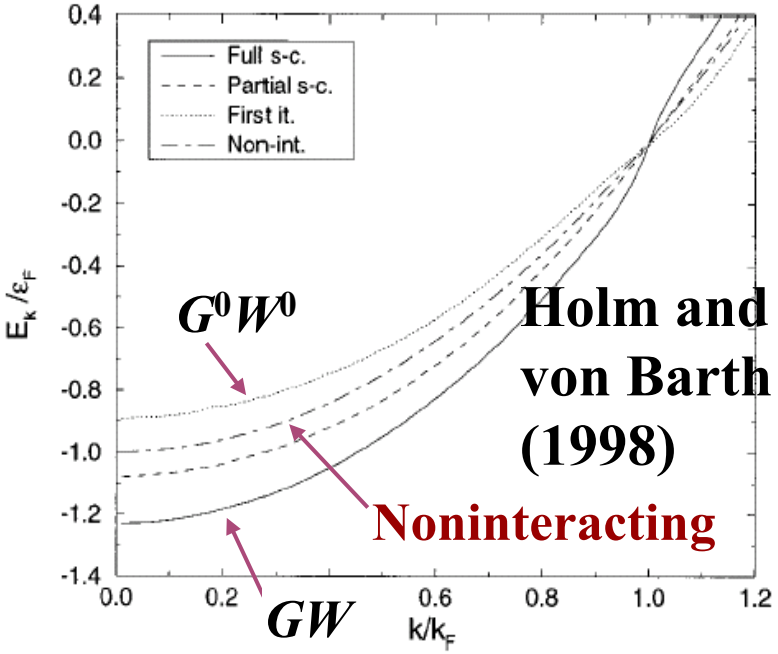

DOS in real materials often worse than LDA

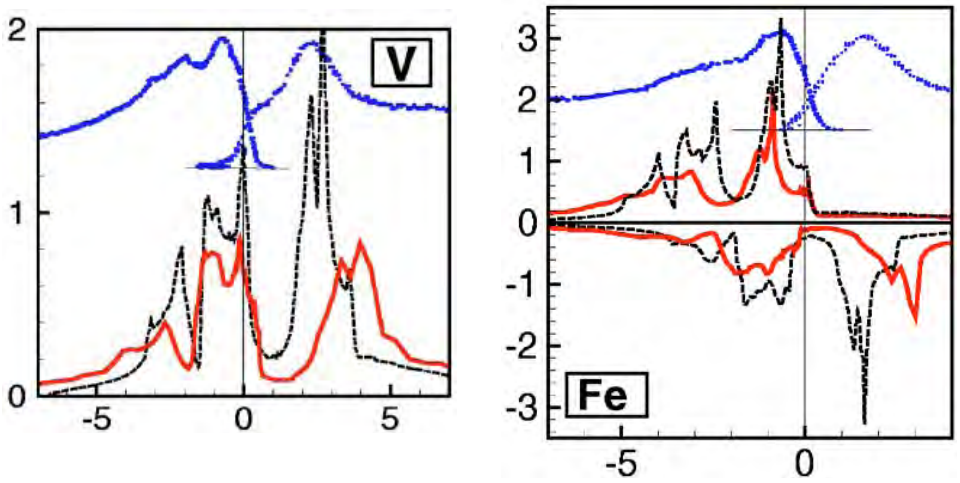

From Belashchenko et al, PRB 73, 073105

Quasiparticle Self-Consistency

Partition H into $H_0 + \Delta V$ and (noninteracting + residual) in such a way as to minimize ΔV :

$$G_0 = \frac{1}{\omega - H_0} \xrightarrow{GWA} G = \frac{1}{\omega - \left(H_0 + \Delta V(\omega)\right)}$$

$$\left(\omega - (H_0 + \Delta V(\omega))\right) G(\omega) = \delta(\mathbf{r} - \mathbf{r}')$$

We seek the $G_0(\omega)$ that most closely satisfies Eqn. of motion

$$\left(\omega - (H_0 + \Delta V(\omega))\right) G_0(\omega) \approx \delta(\mathbf{r} - \mathbf{r}')$$

$$\rightarrow \Delta V(\omega) G_0(\omega) \approx 0$$

If the GWA is meaningful, $G_0 \approx G$

Q: How to find G_0 that minimizes $\Delta V\, G_0$?

Optimal G_0

Start with some trial V_{xc} (e.g. from LDA, or …). Defines G_0 :

$$H_0 = \frac{-1}{2m}\nabla^2 + V^{\text{ext}}(\mathbf{r}) + V^{\text{H}}(\mathbf{r}) + V^{\text{xc}}(\mathbf{r},\mathbf{r}')$$

$$H_0\psi_i = E_i\psi_i \longrightarrow G_0(\mathbf{r},\mathbf{r}',\omega) = \sum_i \frac{\psi_i(\mathbf{r})\psi_i^*(\mathbf{r}')}{\omega - E_i}$$

GWA determines ΔV and thus H :

$$G_0 \xrightarrow{RPA} \varepsilon(iG_0G_0) \xrightarrow{GWA} \Sigma(\mathbf{r},\mathbf{r}',\omega) = iG_0W; \qquad \Delta V = \Sigma - V^{\text{xc}}$$

Find a new V^{xc} that minimizes norm M, a measure of $\Delta V\, G_0$.

$$V^{\text{xc}} = \frac{1}{2}\sum_{ij}\langle\psi_i|\text{Re}\left(\Sigma(E_i)+\Sigma(E_j)\right)|\psi_j\rangle$$

(approximate) result of min M

Iterate to self-consistency.

At self-consistency, E_i of G matches E_i of G_0 (real part).

Z-factor cancellation

Exact $\Sigma = iGW\Gamma$. Suppose W is exact. Then

$$G = \frac{1}{\omega - H_0 - \left[-V^{xc} + \Sigma(\omega_0) + (\partial\Sigma/\partial\omega)_{\omega_0}(\omega - \omega_0)\right] + i\delta}$$

$$Z = (1 - \partial\Sigma/\partial\omega)^{-1}$$

Residual of this pole (loss of QP weight) is reduced by Z

Write G as $G = ZG^0 + (\text{incoherent part})$ Ward identity

$\therefore GW\Gamma \approx G^0 W + (\text{incoherent part})$ $\Gamma \to Z^{-1}$ for $q', \omega' \to 0$

Similar argument for W. Ishii et al (arxiv 1003.3342)
reversed argument: postulate Γ that satisfies Ward Identity

$$\Gamma_{WI}(p, p+q) \equiv \frac{G(p+q)^{-1} - G(p)^{-1}}{G_0(p+q)^{-1} - G_0(p)^{-1}}$$

Results from $GW\Gamma_{WI}$ similar to G_0W_0.

Formal Justification of QSGW

Our justification for QSGW: find the G_0 which miminizes the difference $\langle G-G_0 \rangle$, according to some definition of $\langle \ldots \rangle$, within the GW approximation.

Why not just find G_0 that minimizes the RPA total energy E^{RPA} ?

$$\frac{\delta E^{\mathrm{RPA}}}{\delta G_0} = 0$$

Not possible … there is no lower bound (PRB76, 165106).

Justifying quasiparticle self-consistent schemes via gradient optimization in Luttinger-Ward theory

arXiv:1406.0772

Sohrab Ismail-Beigi

A different justification (Ismail-Beigi)
Minimize square of *gradient* of Luttinger Ward energy

$$|D|^2 \rightarrow \min \quad \text{where} \quad D = \frac{\delta F[G_0]}{\delta \Sigma}$$

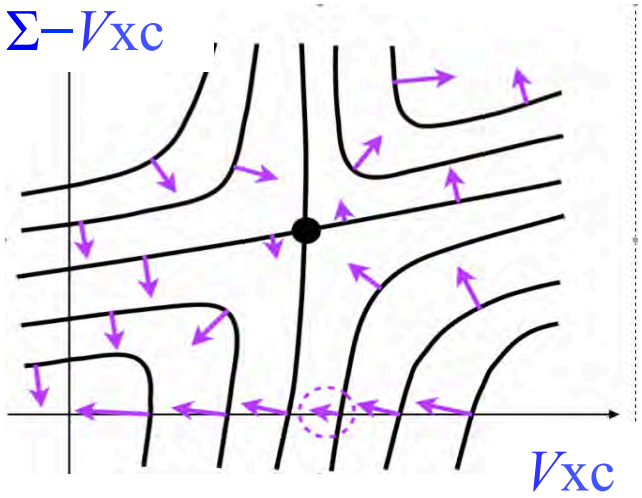

Quasiparticle Self-Consistency for NiO

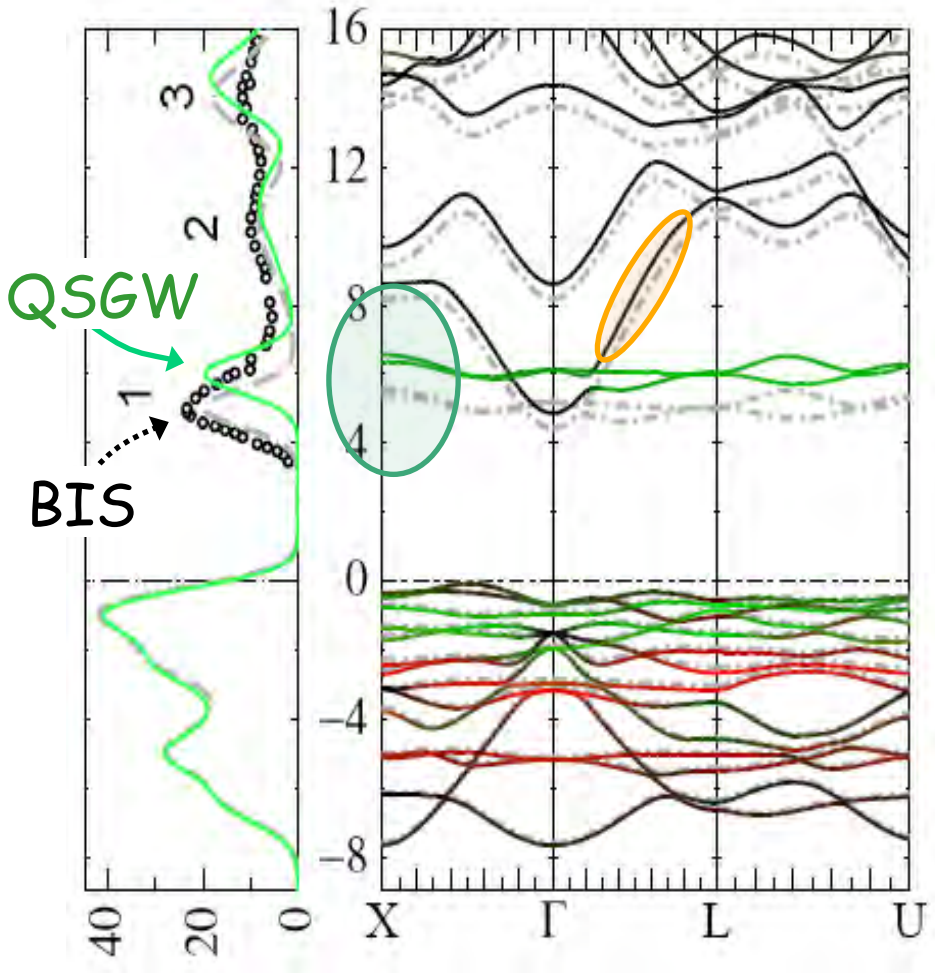

NiO looks good. Gaps a little too big (explain later)

Universal property of QSGW

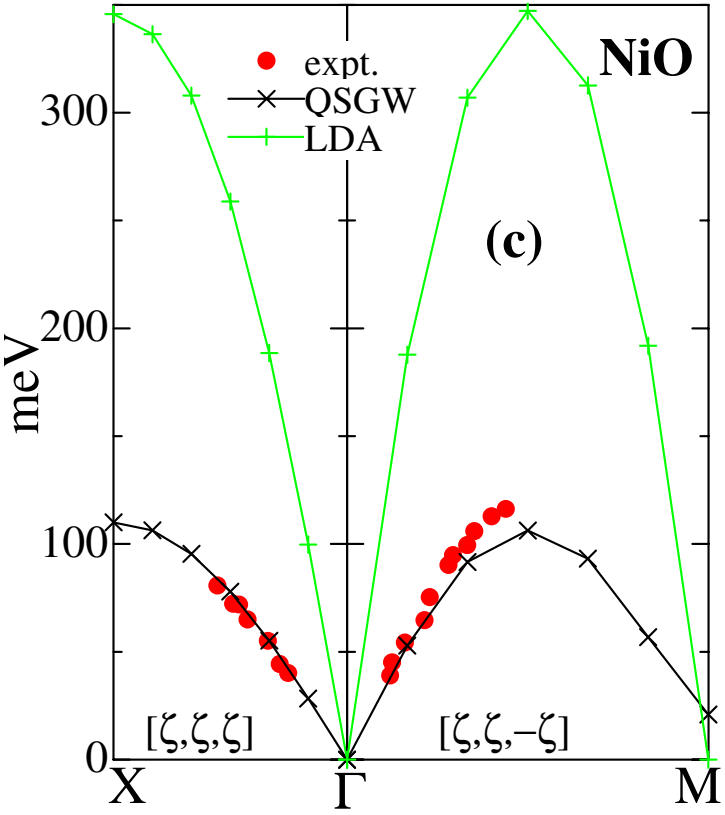

J. Phys. Cond. Matt. 20, 95214

Spin waves in MnO and NiO very well described.

Nothing adjustable, all electrons on same footing.

Fermi Surface for Archetypal *d* system: Fe

Lonzarich Interpretation: "Electrons at the Fermi Surface"

Compare to de Haas-van Alphen data:

FS		dHvA [110]			dHvA [111]	
pocket	QSGW	expt[15]	ΔE_F	QSGW	expt[15]	ΔE_F
I	3.355	3.334	0.01	3.63	3.5342	0.04
II				3.694		
III	0.214	0.319	0.05	0.1627	0.2579	0.06
IV	0.090	0.118	0.04	0.0846	0.1089	0.02
VI	0.318	0.556	-0.13	0.2799	0.4986	-0.14
VII	0.015	0.041	0.04			

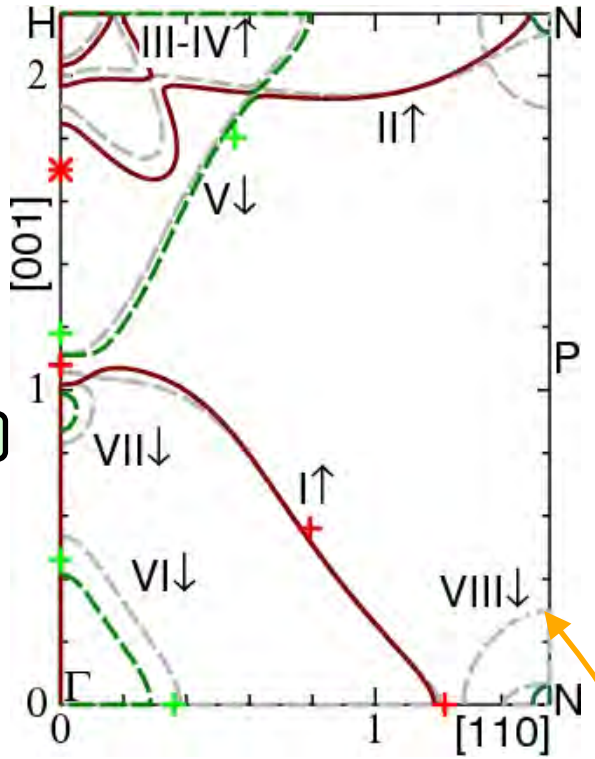

1. Estimate QSGW $\Delta E^{QP} \sim \Delta E_F$ assuming band shifts rigidly
2. Agreement ~0.05 eV except for VI pocket (next slide)
3. LDA (---) mostly similar except for VIII pocket at N.

Electron-Phonon Renormalization

FS	dHvA [110]			dHvA [111]		
pocket	QSGW	expt[15]	ΔE_F	QSGW	expt[15]	ΔE_F
VI	0.318	0.556	-0.13	0.2799	0.4986	-0.14

The electron-phonon interaction renormalizes v_F in a window $E_F \pm 50$ meV. Customary to write as $v_F = (1+\lambda)\, v_F^0$

λ scales as ~ $1/v_F$ in e.g. Thomas -Fermi model for a spherical surface:

$$\lambda_{TF} = \frac{e^2}{\hbar v_F}\left[\frac{1}{2}\ln\frac{k_{TF}^2}{k_{TF}^2+k_F^2} + \frac{k_F}{k_{TF}}\arctan\frac{k_F}{k_{TF}}\right]$$

Compare to experimental cyclotron m^*

	m^*/m [110]			m^*/m [111]		
	QSGW	LDA	expt[17]	QSGW	LDA	expt[17]
I	2.5	xxx	2.6			
V				-1.7	xxx	-1.7
VI				2.0	xxx	2.8

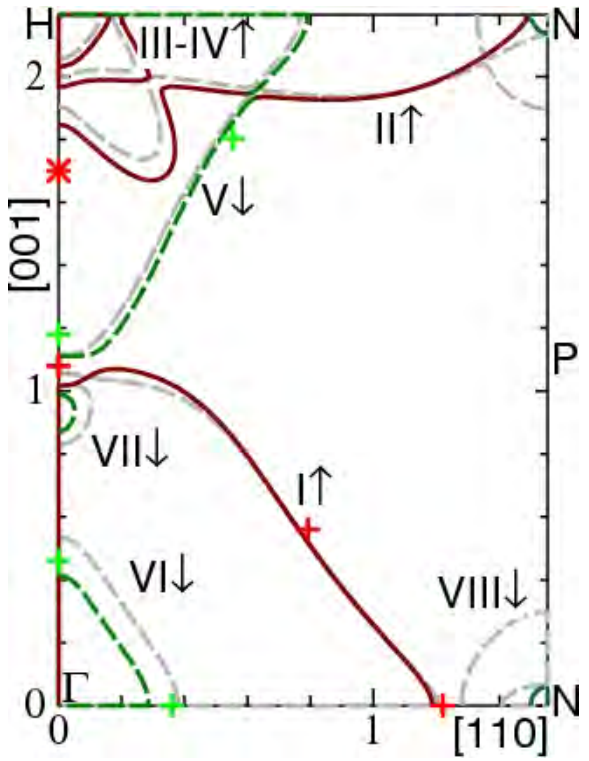

$\lambda \approx \lambda_{TF} = 0.6$ for pocket VI, small for others

$m^{*,GW}/m^{*,cyc} \approx 1$ except for pocket VI ... λ_{TF} explains discrepancy

Compare to ARPES measurement of Fe

ARPES expt by Schafer et al, PRB72, 155115 (2005):

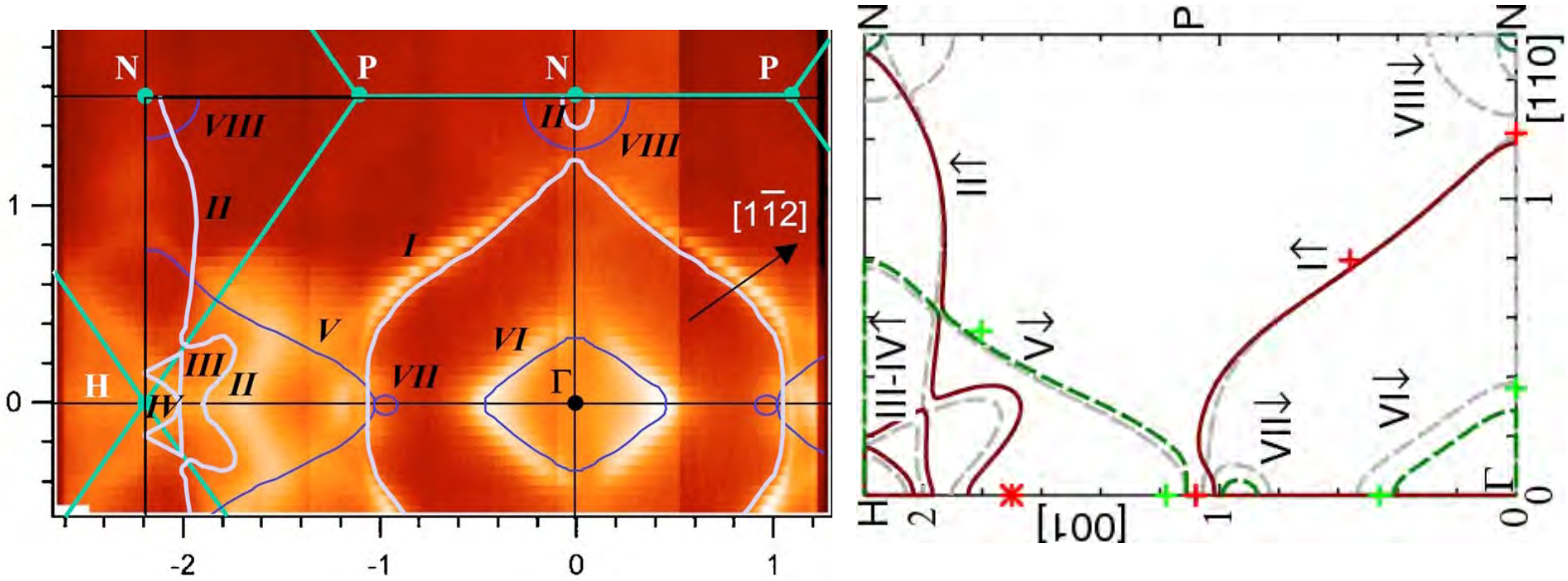

1. High quality sample : thin film of Fe (few dislocations)
2. High photon energy (139eV) – final states nearly parabolic and long penetration depth

Few systems with comparable experimental conditions

Compare ARPES to QS*GW* $E(\mathbf{k})$

QS*GW* $E(\mathbf{k})$ match to ARPES and inverse PE (Santoni & Himpsel, Phys. Rev. B 1991) very well, but …

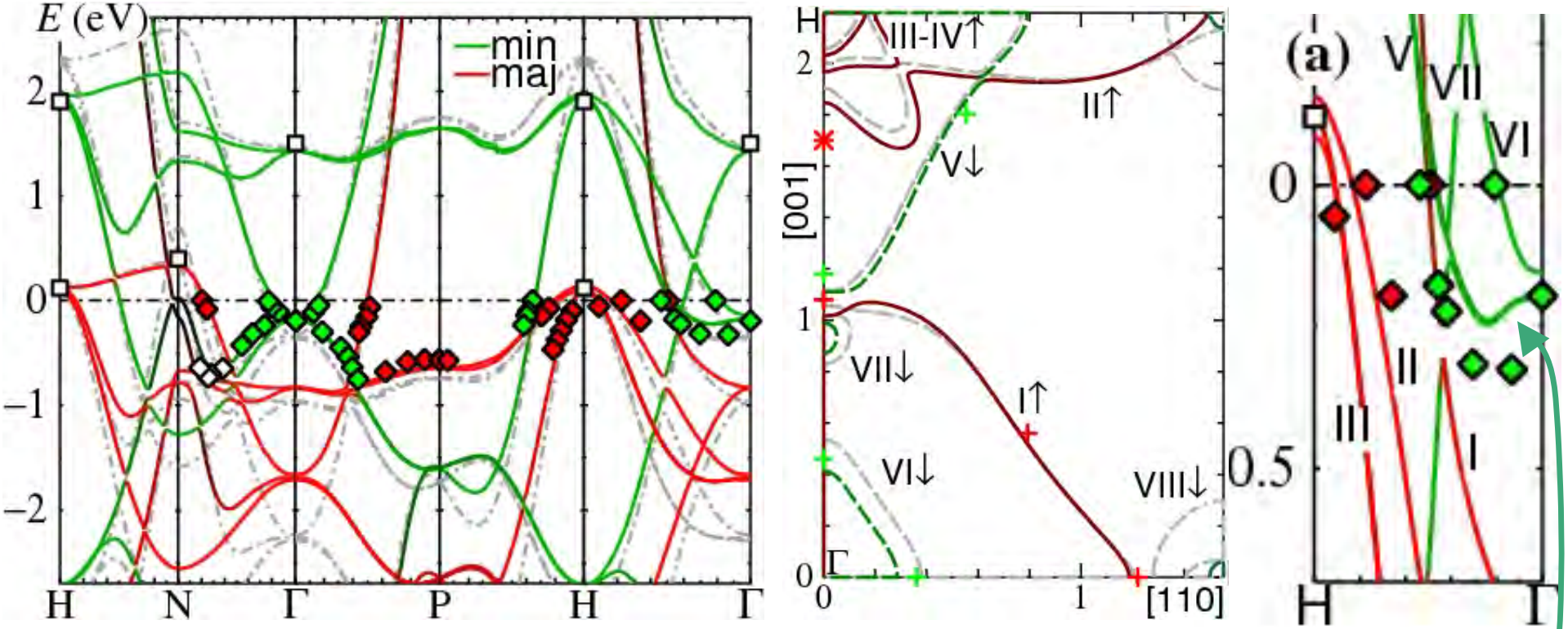

Much better than LDA. But discrepancies at sub 0.1 eV scale:

the VI ↓ dispersion is different near $\mathbf{k}=0$

the II ↑ crosses E_F at a slightly different point (*).

Simulation of ARPES Measurement

Pendry: e^- scatter as they propagate to the surface, smearing out the final state $\mathbf{k}_f$.

$$A_f(\mathbf{k}_\perp) = \frac{\Delta k_\perp / 2\pi}{(\Delta k_\perp / 2)^2 + (k_\perp - k_\perp^0)^2}$$

Strocov (J. Elec. Spect. and Rel. Phenomena, 2003): $\mathbf{k}_f \perp$ surface is broadened into a Lorentzian distribution. Extract $\Delta k_\perp$ from measurement.

For $\hbar\omega_{\text{photo}}$~100-130eV, $\Delta k_\perp \approx 0.2\text{Å}^{-1}$ (Feibelman PRB 1974).

Model for ARPES:

$$I^{\text{QSGW}}(\mathbf{k},\omega) \propto \int dk_\perp A_f(\mathbf{k}_\perp + \mathbf{k}) A^{\text{QSGW}}(\mathbf{k}_\perp + \mathbf{k}, \omega)$$

$\mathbf{k}$-broadened final state

QSGW spectral function: ω-broadened QP

Effect of Δk_f on Apparent FS at k=0.77H

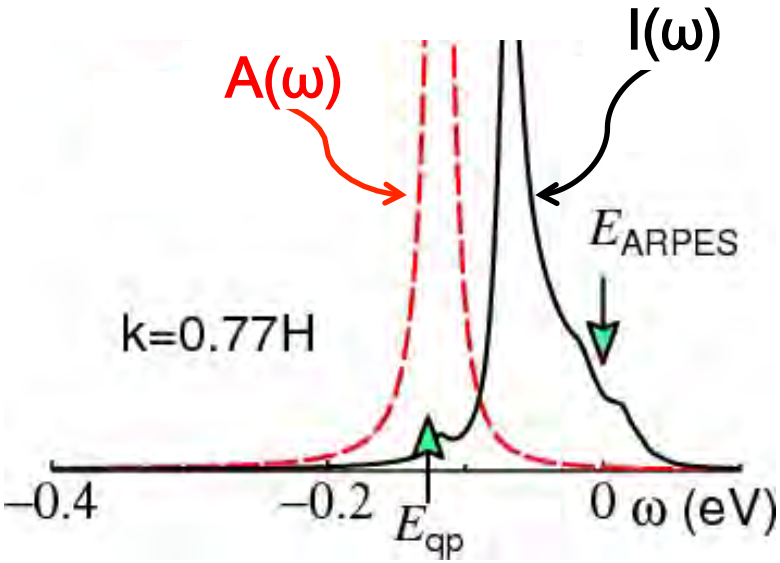

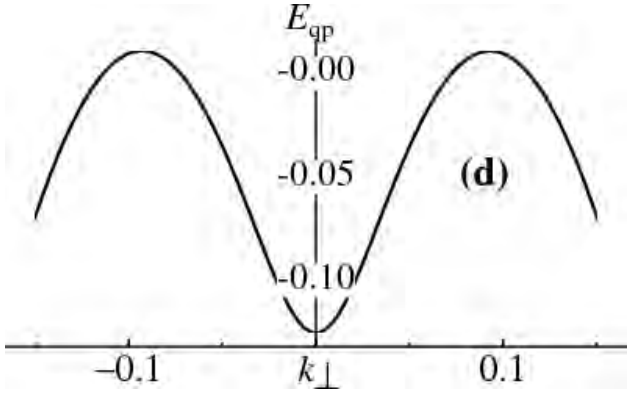

k=(0,0,0.77) is the minimum point on line **k**=($k_\perp/\sqrt{2}$, $k_\perp/\sqrt{2}$,0.77).

A measurement that averages over $k_\perp$ biases the peak closer towards E_F.

Conclusion: ARPES $I(\omega)$ not a direct measure of $A(\omega)$. Suitably interpreted, excellent agreement with QSGW $A(\omega)$.

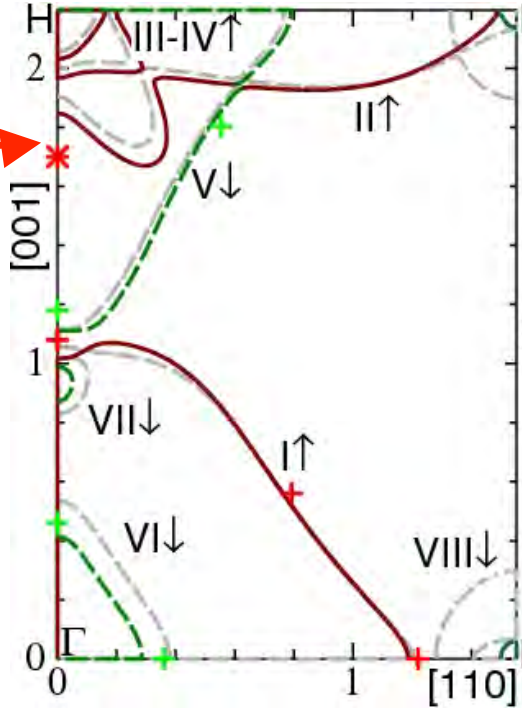

skip

Effect of Δk_f on minority V,VI for k<0.3H

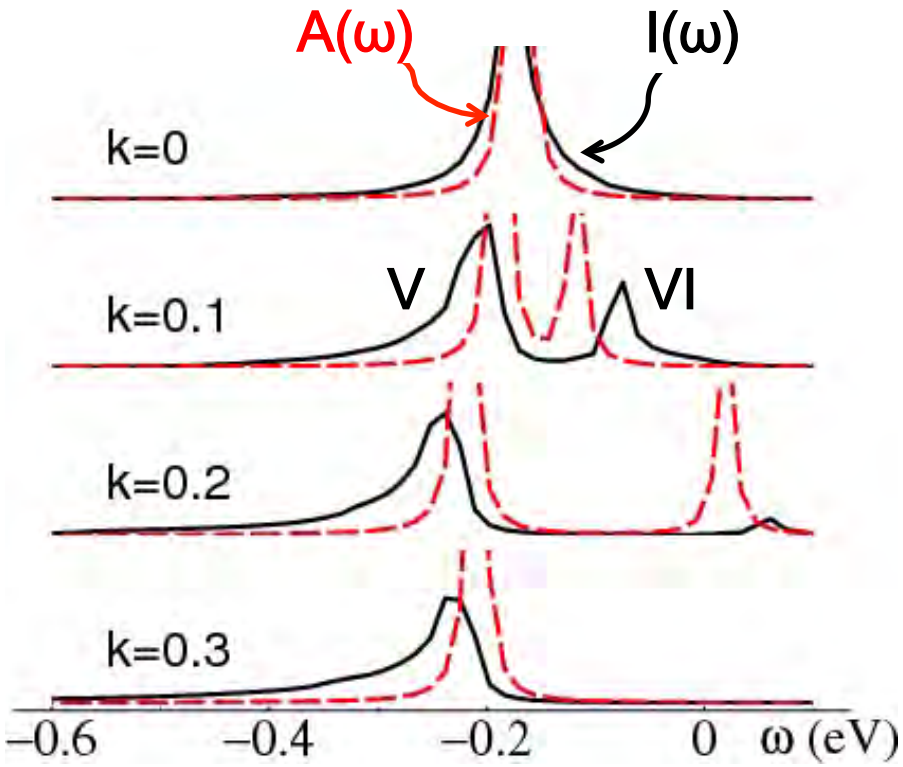

At the Γ-point, peaks in $A(\omega)$ and $I(\omega)$ coincide. QSGW closely matches PES at Γ.

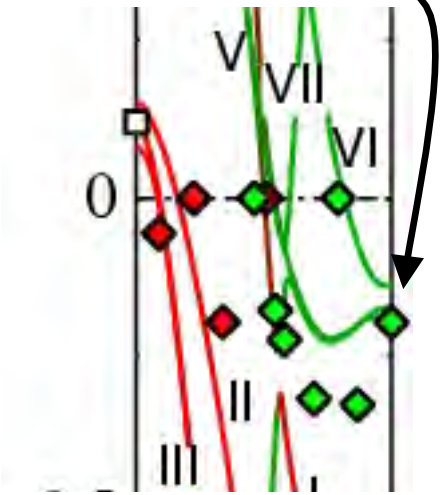

As k increases the peaks separate, and then merge back together.

Conclusion: most of the discrepancy with PES data is an artifact of broadening of the excited final state by scattering.

Fermi velocities in Fe

Compare QSGW v_F to ARPES

Band	Γ-H		Γ-N		Γ-P†	
	QSGW	ARPES	QSGW	ARPES	QSGW	ARPES
I	2.2	1.1	1.6	1.2	3.7	2.4‡
II	0.7	0.7				
V†	1.1	1.1			4.1	2.3‡
VI	0.8	0.7	1.2	0.8	1.3	0.9

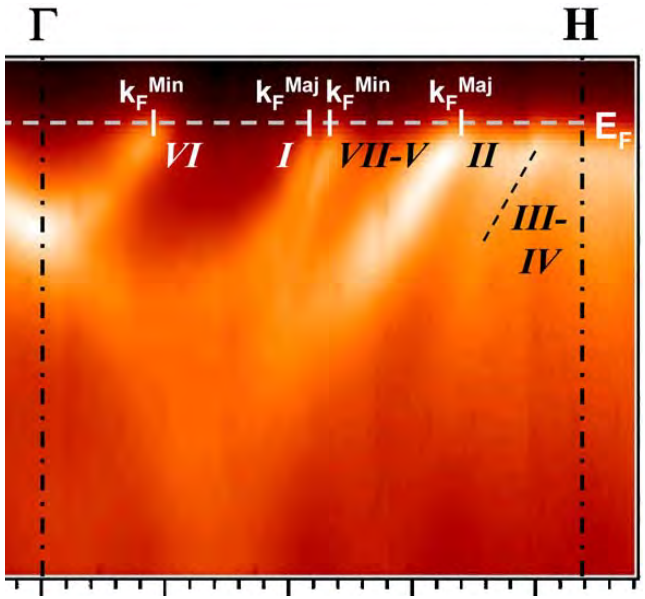

Main point of discrepancy: band I.
This is a very dispersive *sp* band.

… But QSGW matches cyclotron m^* …

	m^*/m [110]			m^*/m [111]		
	QSGW	LDA	expt[17]	QSGW	LDA	expt[17]
I	2.5	xxx	2.6			
V				-1.7	xxx	-1.7
VI				2.0	xxx	2.8

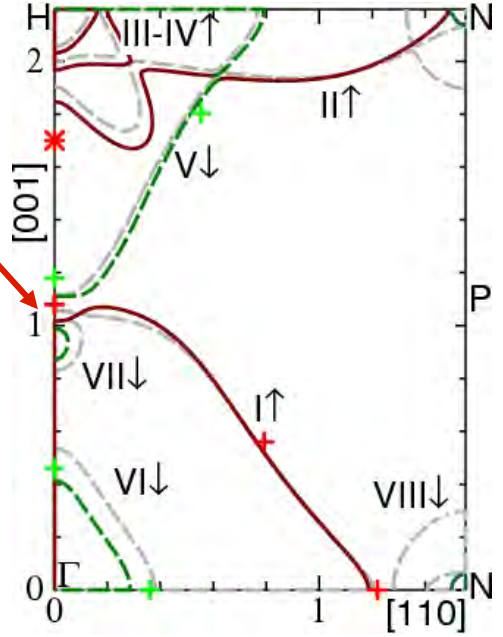

Conclusion: QSGW v_F is more reliable than ARPES measurement

ARPES Measurements of Ni

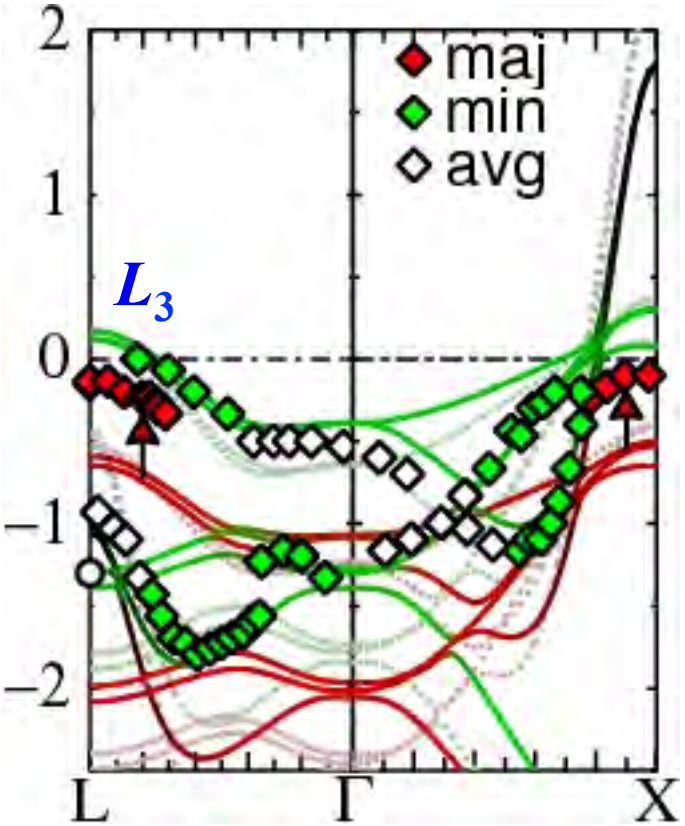

W^{RPA} is screened in the charge channel only … no spin fluctuations.

QSGW : vast improvement over LDA for TM in general. But for Ni, problems appear

Calculated ΔE_x :

QSGW	LDA
0.76	**0.71**

Calculated M :

QSGW	LDA
0.76	**0.60**

Trends in 3*d* series

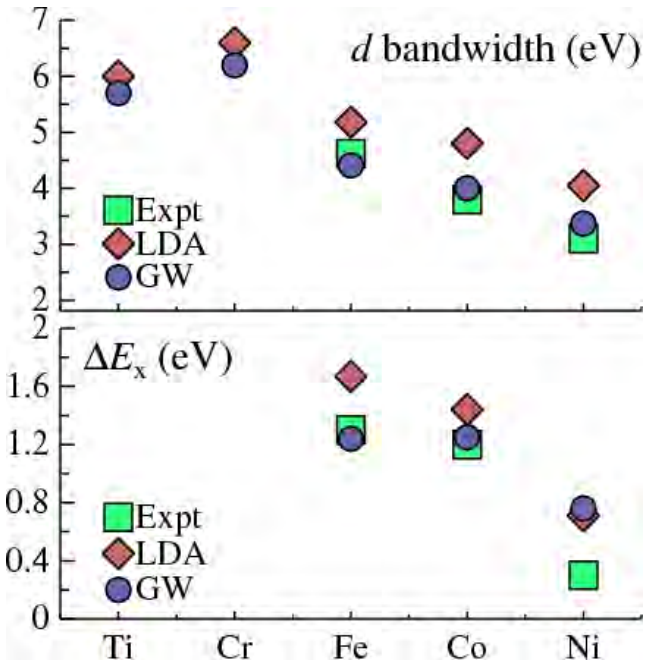

Spin Fluctuations

In Ni spin fluctuations are important (Nolting et al, 1989)
Quite generally, QSGW appears to:

- predict $\boldsymbol{M}$ in local-moment systems very well
- overestimate $\boldsymbol{M}$ in itinerant systems.

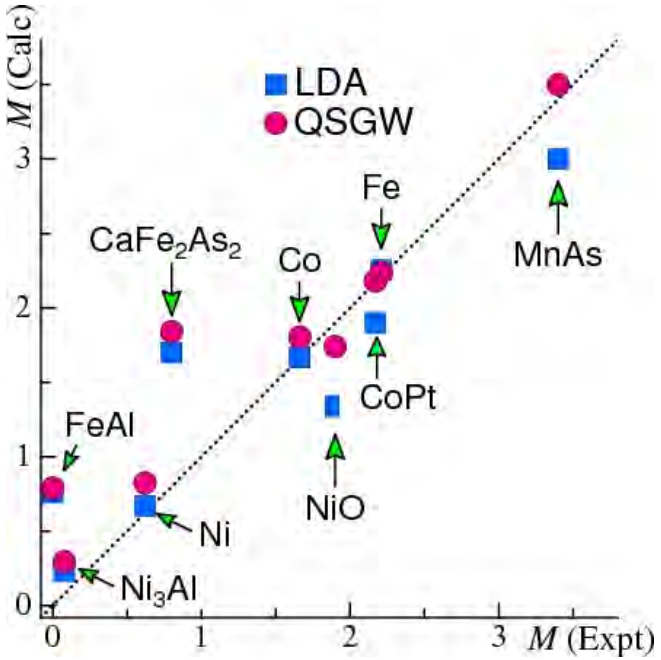

LDA has two distinct errors:
$\langle \boldsymbol{M} \rangle$ is too large in itinerant materials.
$\langle \boldsymbol{M} \rangle$ is too small in local-moment systems (CoPt, MnAs)
In Ni the errors cancel …
$\langle \boldsymbol{M} \rangle$ is fortuitously good!

Spin fluctuations reduce $\langle \boldsymbol{M} \rangle$. Moriya estimated $\langle \Delta \boldsymbol{M} \rangle$ from FD theorem. Requires $\int d\omega \, \mathrm{Im}\chi$ (Mazin et al PRL 2004).
… Better fluctuations are built into higher order diagrams.

Renormalization of ΔE_x

- If Ni is reasonably described by a QP picture, fluctuations will modify the static (QS*GW*) 1-body B^{sf}.
- Simulate (for now) by adding an external static B^{sf} to the QSGW potential, iterate QS*GW* + B^{sf} to self-consistency.

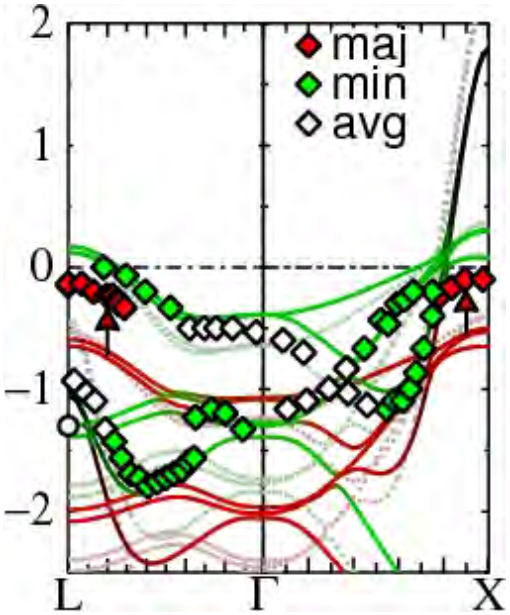

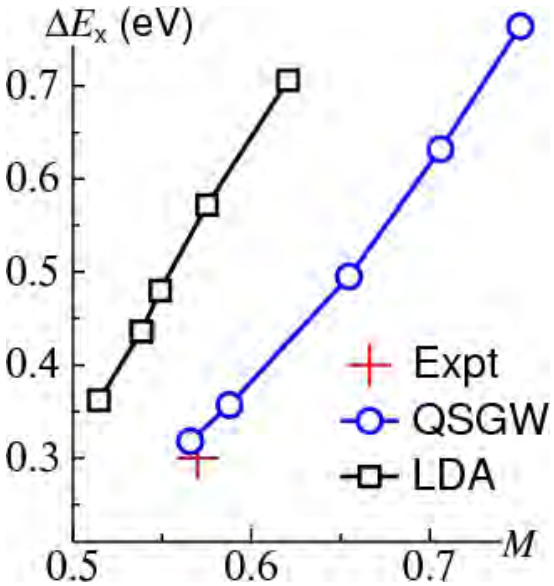

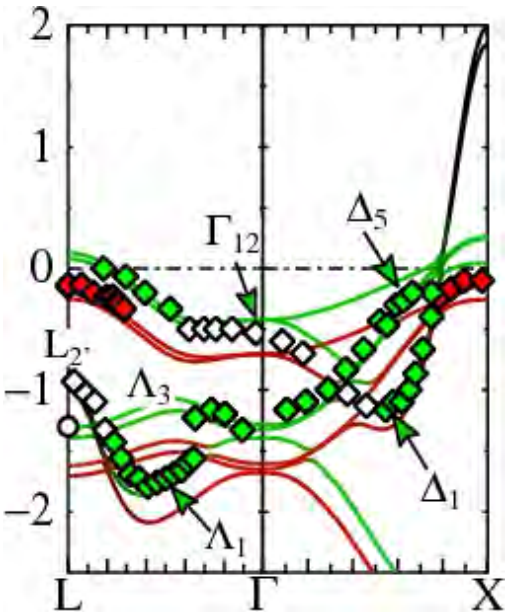

$B^{sf}=0$

B^{sf} at $\langle M \rangle = \langle M^{expt} \rangle$

La_2CuO_4

LSCO : antiferromagnetic insulator, gap ~2 eV
Nonmagnetic calculation: LSCO is metal with Cu x^2-y^2 at E_F.

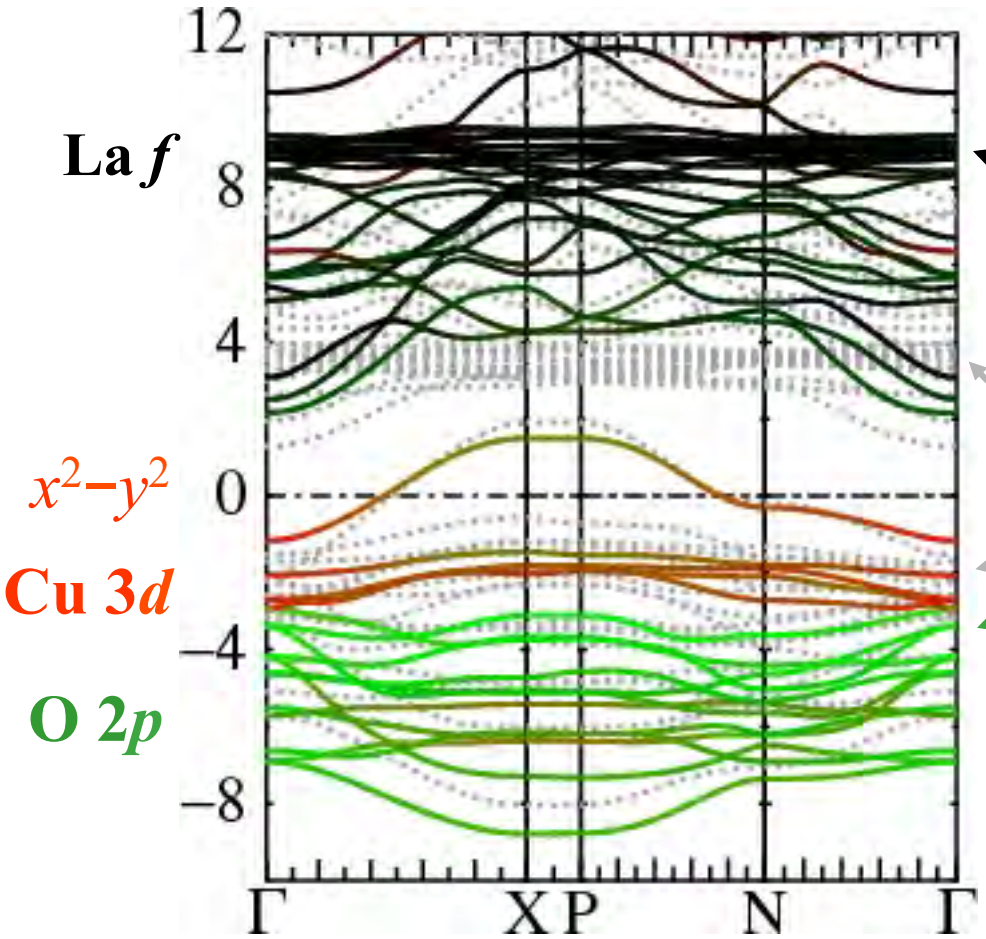

Significant intermixing of O $2p$ with Cu $3d$.

Failings of LDA:

- La $4f$ states much too low.
- O $2p$ ~1.3 eV too shallow
  Too much O $2p$ admixes into Cu x^2-y^2 .
- Ordered antiferro state is still a metal

LDA+DMFT:
Opens a gap of order 2 eV

QSGW La_2CuO_4 ordered antiferromagnetic state

Low T° phase: AFM with (π, π) ordering

QSGW: insulating state with E_g~4eV.

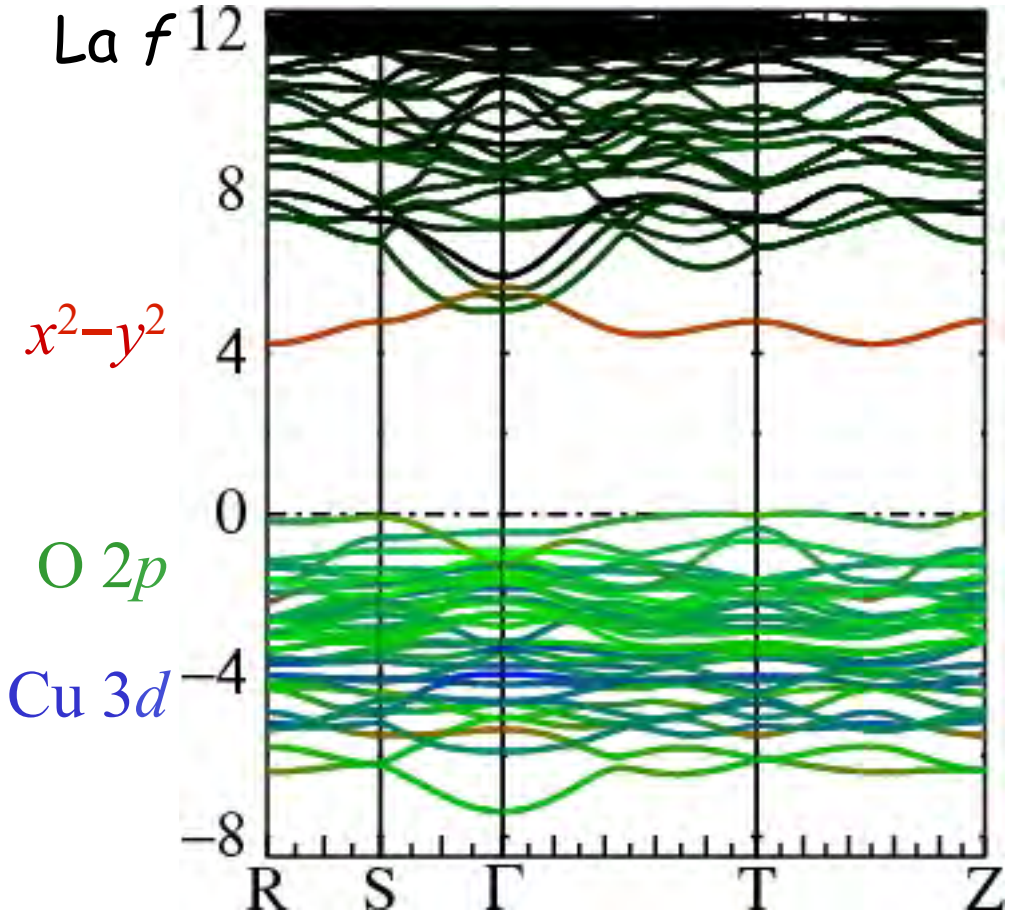

Results:

- Lowest CB is Cu x^2-y^2 with significant O 2p admixed.
- VBM is O 2p.
- Cu x^2-y^2 ↑ and ↓ split by ~10eV
- Remaining Cu *d* pushed below O 2p.
- Magnetic moment M~0.8.

Failings:

- Gap ~4eV >> expt (2 eV)
- Disorder is expensive

CoO shows a pattern very similar to La_2CuO_4 ….

AFM II spin configuration:

The 5 $Co^{\uparrow}$ states are filled

The 5 $Co^{\downarrow}$ states split into 3(occ)+2(unocc) separated by a gap.

The QS*GW* gap (4.4 eV) is 2 eV too big (experiment ~2.4 eV).

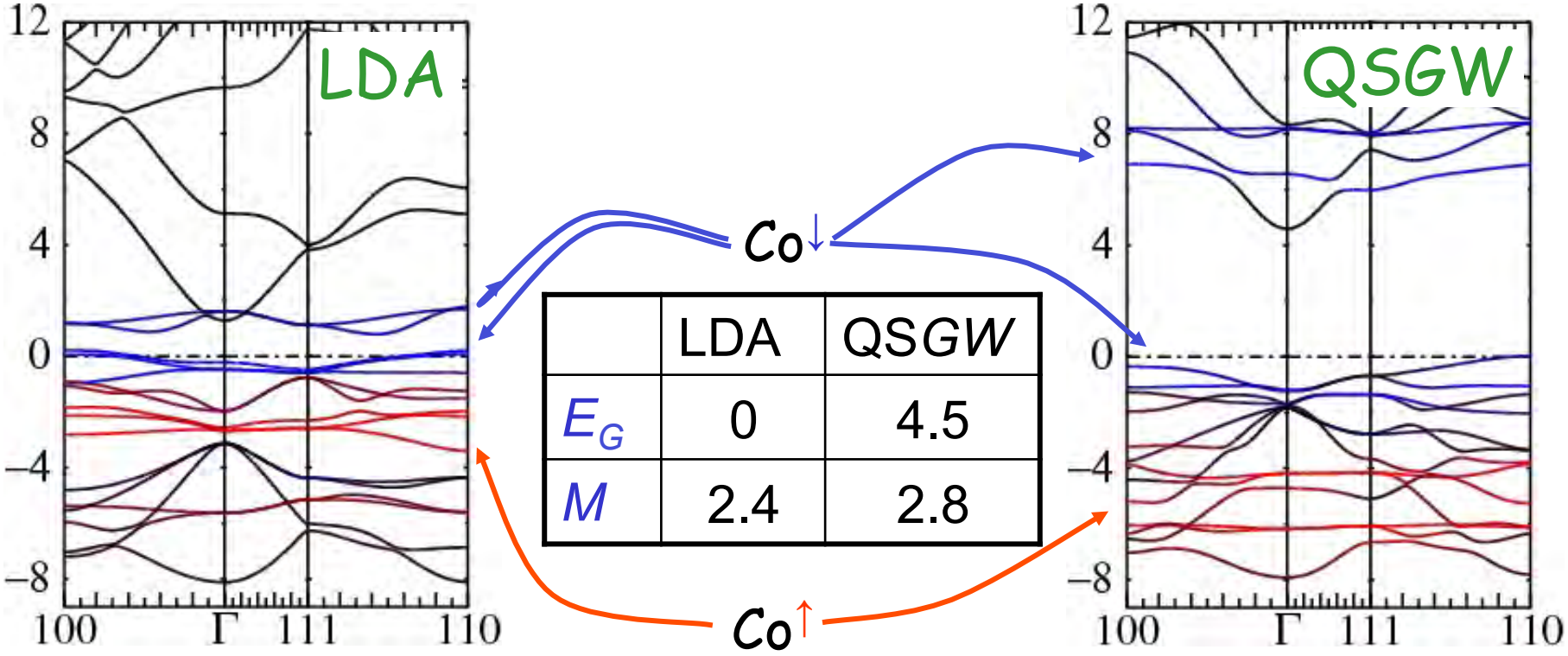

	LDA	QS*GW*
E_G	0	4.5
M	2.4	2.8

LDA: a stable AFM state with no gap (TR symmetry).

The O(2p) – Cu (3d) alignment is ~2 eV different from GW

… where NiO does not

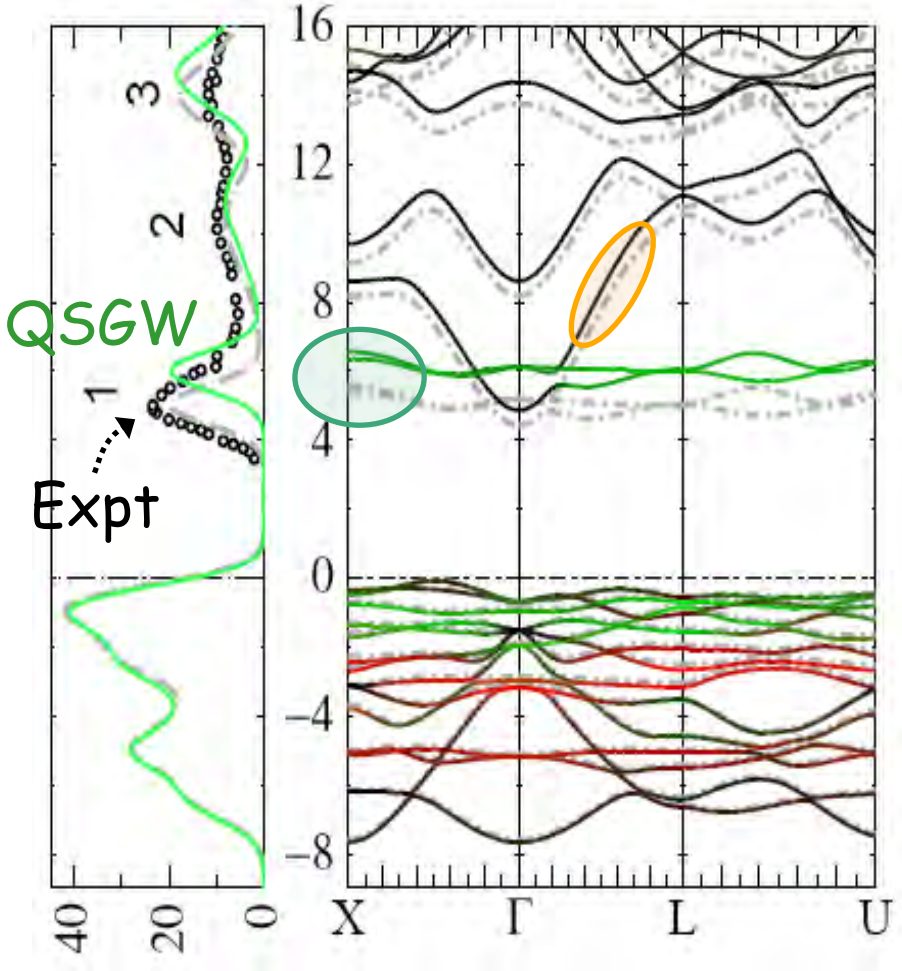

The BIS spectra show 3 distinct peaks:

- 1 near 4.5 eV (Ni *d*)
- 2 near 10 eV (O *sp*)
- 3 near 14 eV (mixed)

QSGW overestimates :

- 1 by ~1.1 eV (similar to $SrTiO_3$ and many nonmagnetic TM oxides)
- 2 by 0.3 eV (similar to *sp* semiconductors)
- 3 by 0.5 eV.

All of this can be explained
by the ladder diagrams
missing from the RPA polarizability … (next slide)

Why the NiO Bandgap is too large

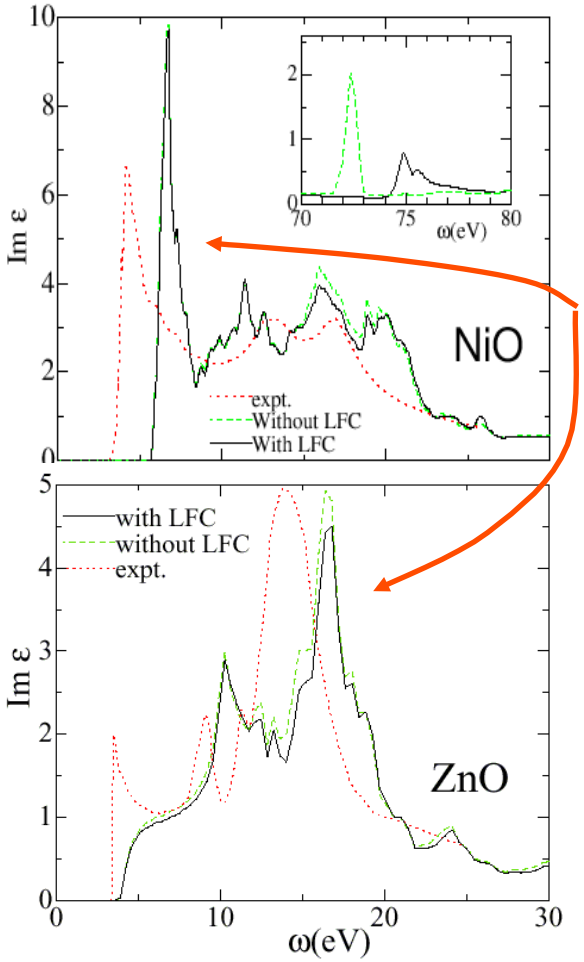

Plasmon peaks in Im $\varepsilon(\omega)$ are too high

This makes $\varepsilon_\infty = \mathrm{Re}\,\varepsilon(0)$ too small

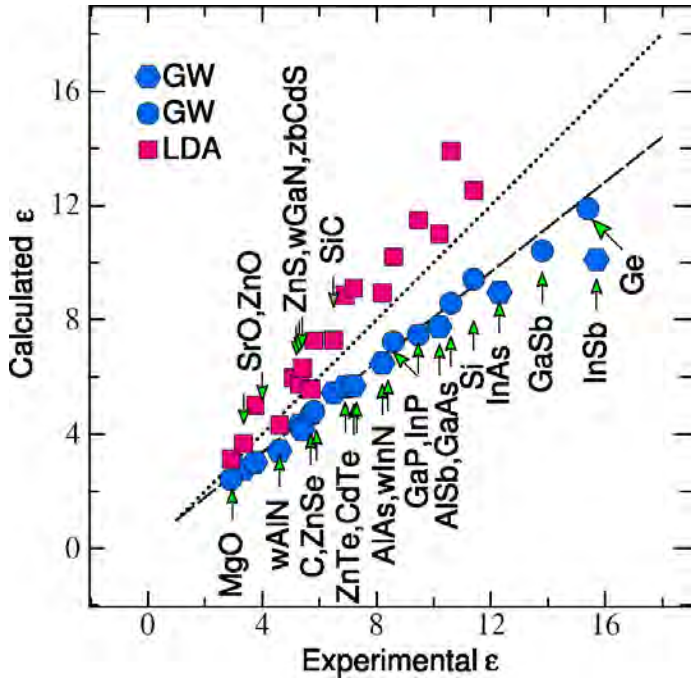

ε_∞ is *universally* 20% too small in insulators (missing ladders)

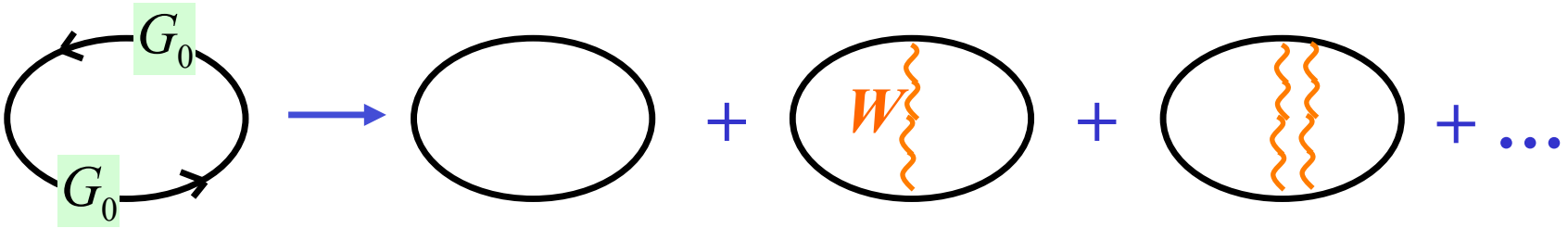

Better screening in the charge channel fixes much

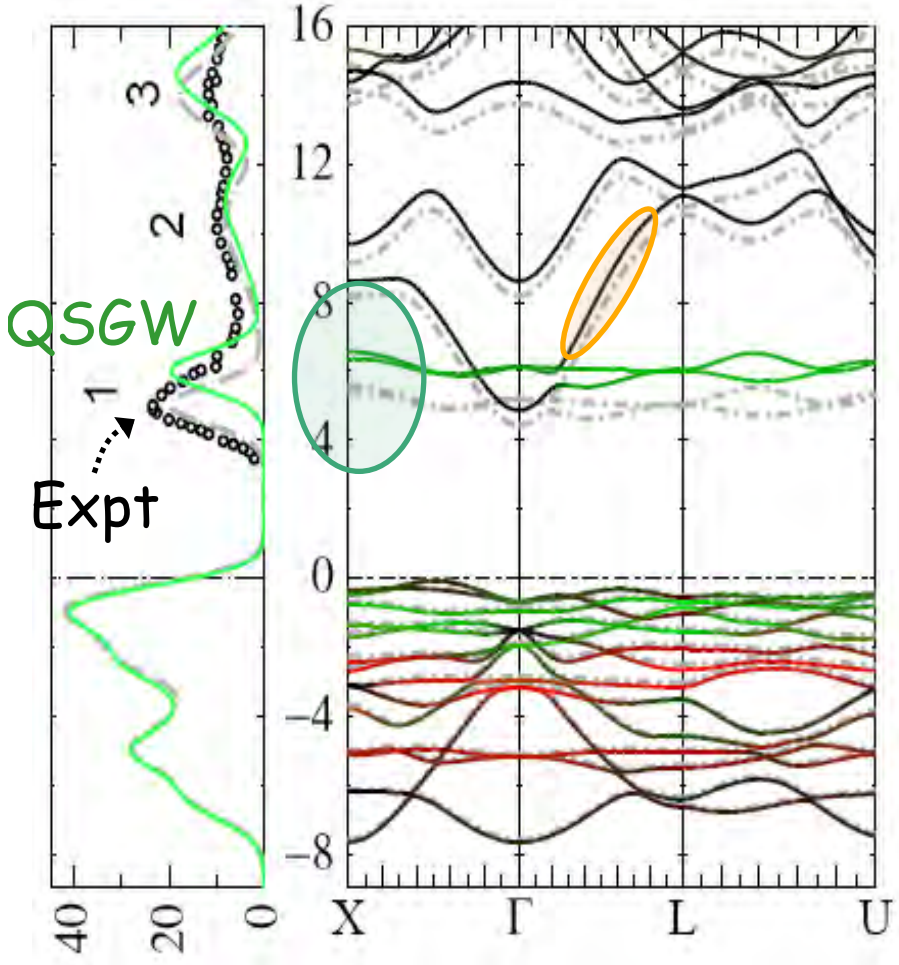

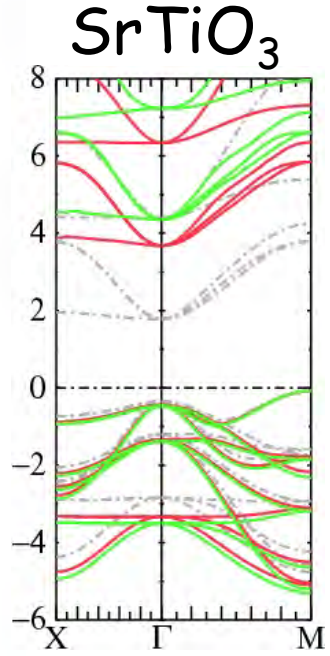

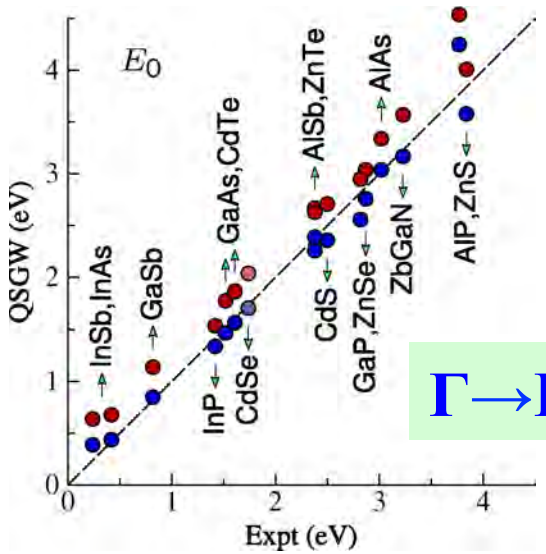

Estimate error

$W \sim [\varepsilon_\infty^{-1}(\text{expt})/\varepsilon_\infty^{-1}(\text{QS}GW)]\, W^{\text{RPA}}$

Result: spectra aligns almost exactly with BIS. Peaks 1, 2, 3 shift different amounts

Seen in most TM oxides and universally seen in *sp* systems

A different kind screening for CoO and La_2CuO_4

For CoO and La_2CuO_4 similar renormalization of W is not enough.

W should be screened in spin channels too. Adds a new $W^{\uparrow\downarrow}$ and modifies $W^{\uparrow\uparrow}$, $W^{\downarrow\downarrow}$ (Katsnelson and Lichtenstein, J. Phys C 11, 1037)

$$\Sigma^{\sigma(ph)}_{1,1'} = G^{\sigma'}_{2,3} W^{\sigma\sigma'}_{12,1'3}$$

$$W^{\sigma\sigma} = U^d \chi^{dd} U^d + U^m \chi^{mm} U^m \pm U^d \chi^{dm} U^m \pm U^m \chi^{dm} U^d$$

$$W^{\sigma\neq\sigma'} = U^m \chi^{\sigma\neq\sigma'} U^m$$

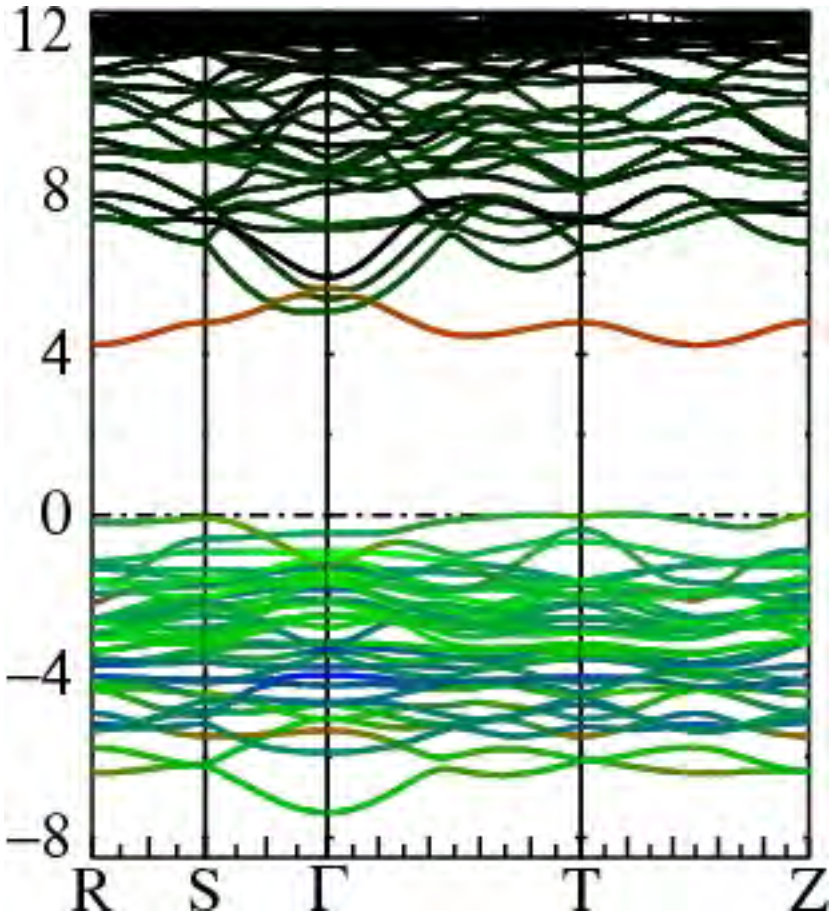

… but is hard to do and other terms may also matter (See Antropov's talk tomorrow)

Nonperturbative Additions to GW diagrams

GW+DMFT: Alternative to low-order diagrammatic theory

VOLUME 90, NUMBER 8 PHYSICAL REVIEW LETTERS week ending 28 FEBRUARY 2003

First-Principles Approach to the Electronic Structure of Strongly Correlated Systems: Combining the *GW* Approximation and Dynamical Mean-Field Theory

S. Biermann,[1,2] F. Aryasetiawan,[3] and A. Georges[2,1]

Formulate theory in terms of free energy functional $\Gamma(G,W)$.
With Dyson equation, solve for (G,W) in terms of (G_0,v) in a 2-step process

$$G^{(1)} = G^{(0)} + G^{(0)}\Sigma^{(1)}G^{(1)} \qquad W^{(1)} = v + vP^{(1)}W^{(1)}$$

$$G^{(2)} = G^{(1)} + G^{(1)}\Sigma^{(2)}G^{(2)} \qquad W^{(2)} = W^{(1)} + W^{(1)}P^{(2)}W^{(2)}$$

Do stage (1) at GW level for whole system;
Do stage (2) at high level for a subsystem you select.

A QPGW+DMFT study of La_2CuO_4

- New QPGW+DMFT performed at Rutgers (Choi, Kutepov, Kotliar, Haule) See arXiv: 1504.07569
- QPGW is intermediate between COHSEX and QSGW

$\Sigma(\omega)$ is linearized: $\Sigma^{lin}(\omega) = \underbrace{\Sigma(0)}_{\text{COHSEX}} + \underbrace{\omega\,\Sigma'(0)}_{\text{Linear term}}$

Quasiparticlize $\Sigma^{lin}(\omega) \rightarrow [\Sigma^{lin}(\omega_i) + \Sigma^{lin}(\omega_j)]/2$

Σ^{lin} increases without bound ⇒ QPGW should underestimate gaps , while COHSEX should overestimate them

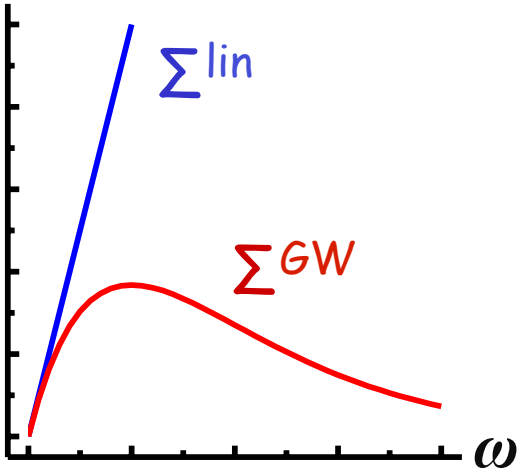

	QSGW	scGW	QPGW
E_G	4.0	4.0	3.5
M	0.8	0.8	0.8

skip

On the QPGW+DMFT Implementation

1. carry out a QPGW calculation to self-consistency on the Matsubara axis and obtain a quasiparticlized G_0

2. Choose a set of local orbitals from maximally localized Wannier functions $\{i\}$ taken from a wide energy window.

3. Use the quasiparticlized G_0 to calculate U_{ijkl} within constrained RPA and extract a static U and J.

4. Project G onto G^{loc} (initially G is the quasiparticlized G_0). Use G^{loc}, U, J as inputs to generate Σ^{loc} from DMFT

--- Steps 5 and 6 are iterated to self-consistency

5. From Σ^{loc} calculate Σ^{DC}.

6. Embed $(\Sigma^{\mathrm{loc}} - \Sigma^{\mathrm{DC}})$ into the quasiparticlized G_0 to construct a new G.

skip

Novel features of QPGW+DMFT

1. The sole input is the projector to the set of localized orbitals.
2. Use a wide energy window (20 eV) so :
   - the orbitals are highly localized (>90% overlap with Cu atomic d orbital)
   - The screening from the bath is greatly reduced so the effective interaction $U(\omega)$ becomes weakly ω-dependent. Replace with $U(\omega)$ with $U(0)$ for the DMFT solver (CTQMC)
   - The hybridization function has an additional contribution (mostly O 2p) which substitutes for the missing screening of U

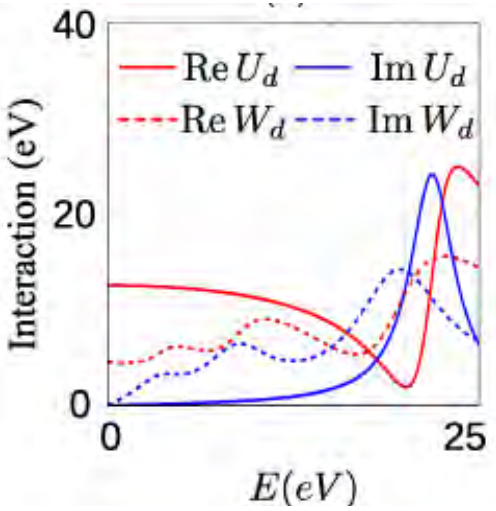

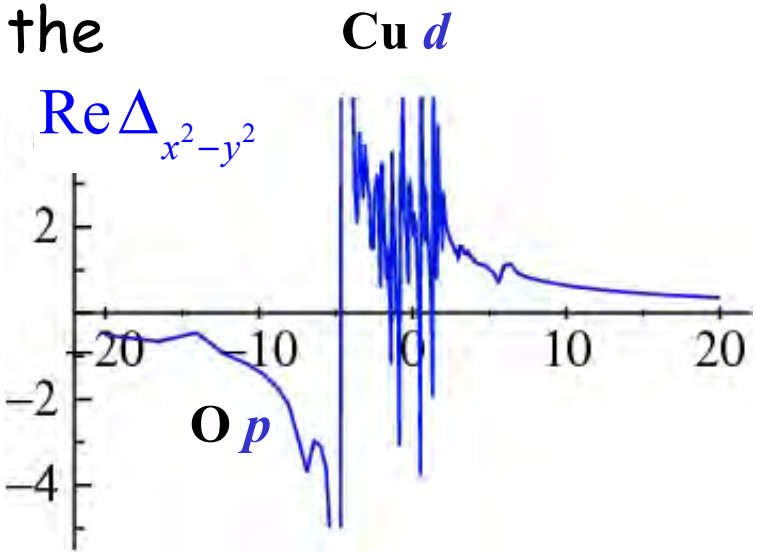

La_2CuO_4 within QPGW+DMFT

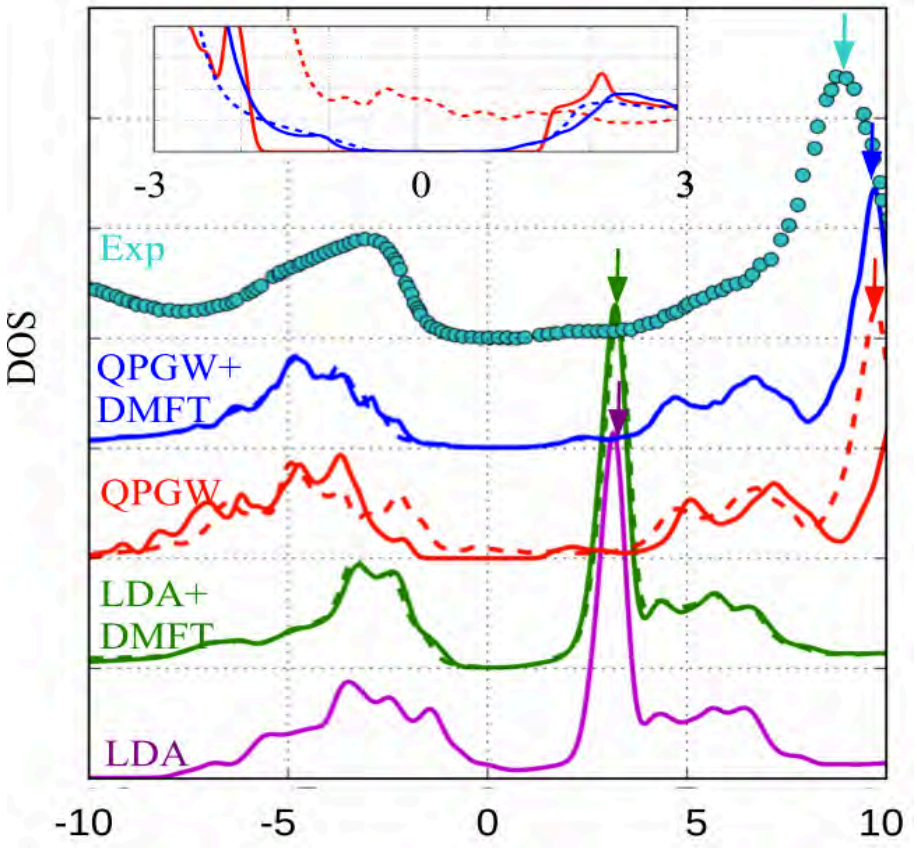

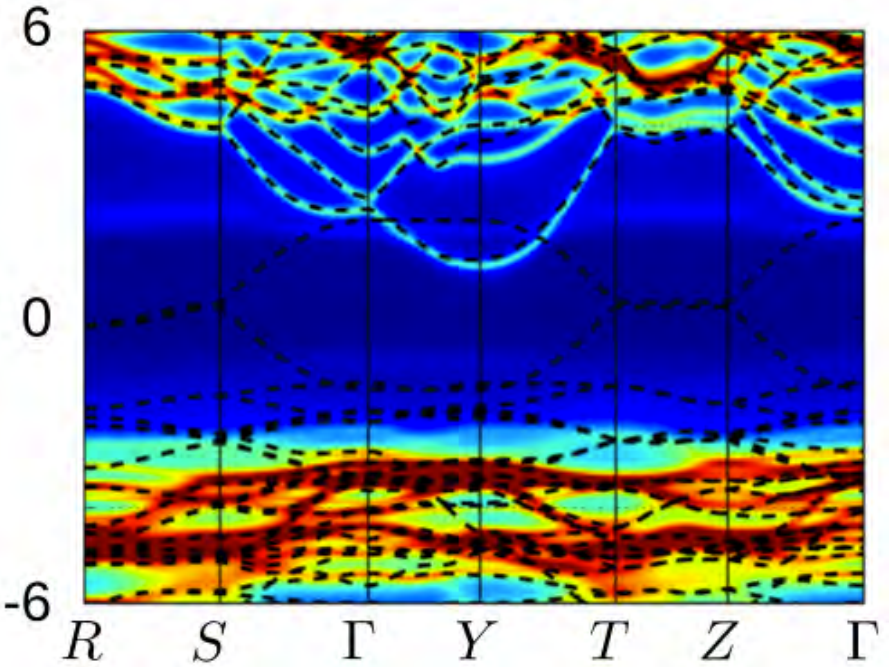

	QP*GW*(A)	QP*GW*(A)+DMFT	QP*GW*(N)+DMFT	Expt
E_G	3.5	1.6	1.5	~2
M	0.7	0.8	0.8	0.4-0.8

Conclusions

1. *GW* provides an *ab initio* framework for optimal G_0, through QS*GW*. QS*GW* dramatically improves the consistency and reliability of G_0 and is universally applicable.
2. QS*GW* alone sometimes sufficient. (ARPES in Fe, SW in NiO, MnO). But spin fluctuations are missing and they can be important (Ni, CoO, La_2CuO_4)
3. LDA+DMFT has been highly successful … but LDA is has serious weaknesses. Results should be much better using QSGW (optimal G_0) for bath.
4. A new QPGW+DMFT approach was developed and applied to La_2CuO_4 . Sums all local graphs, has no empirical input except choice of projector. Reasonable agreement with experiment

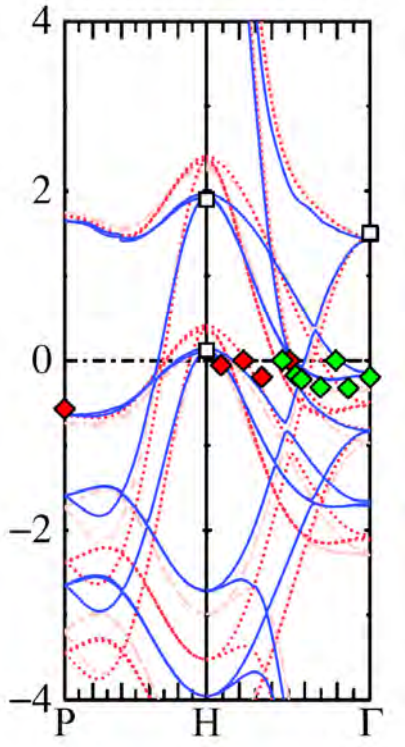

QPGW+DMFT(RPA)

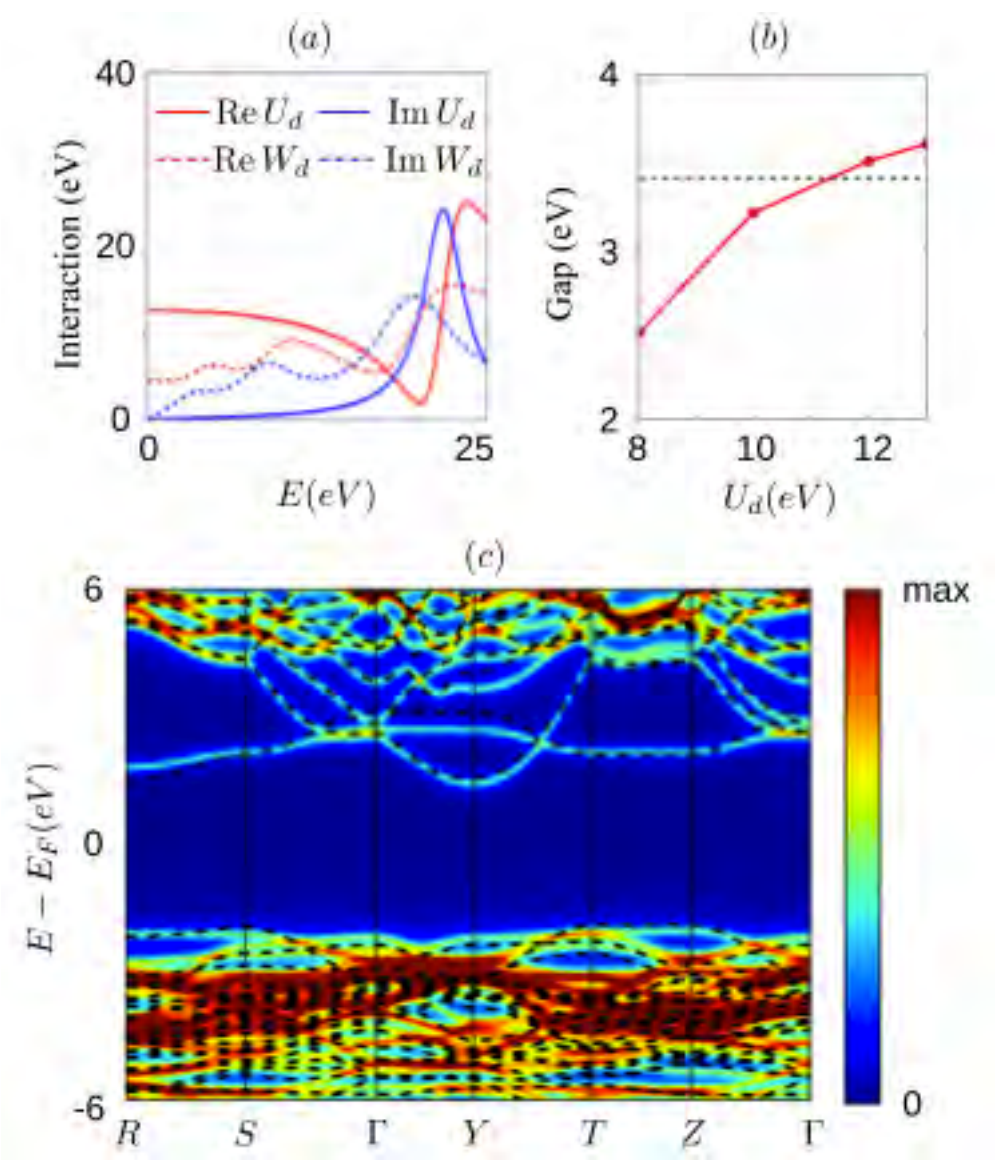

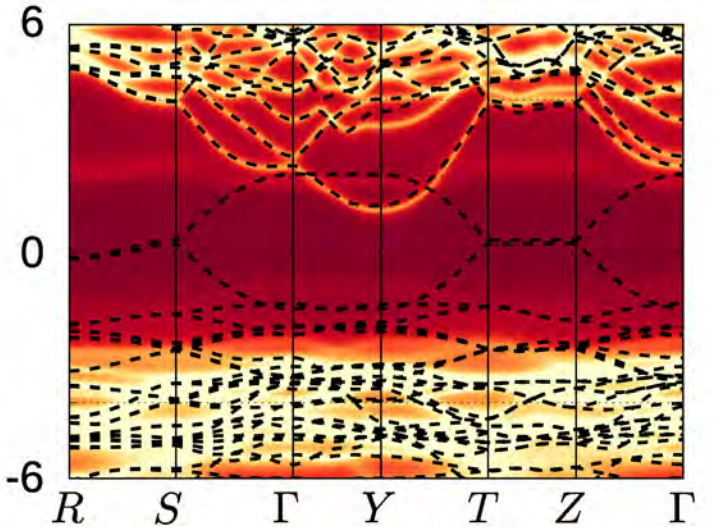

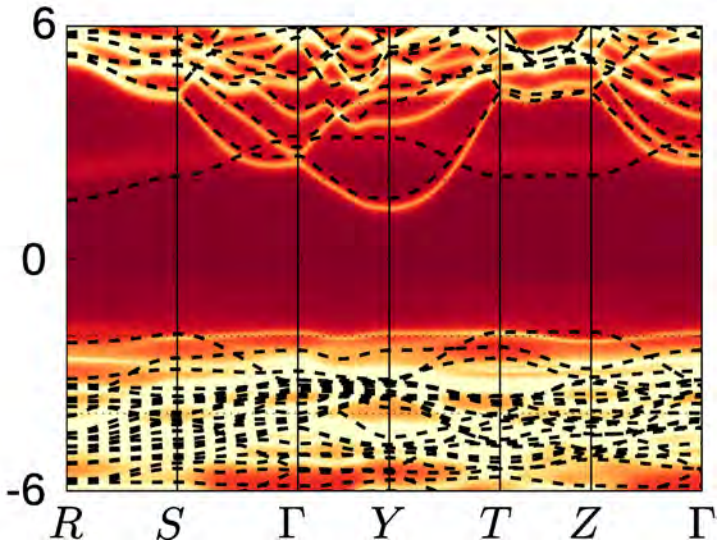

QPGW on an Imaginary Frequency axis

skip

$$\widetilde{G}_{QP}(i\omega_n) = (i\omega_n + \mu - \widetilde{H}_{QP})^{-1}$$

$$\widetilde{\chi}(i\omega_n) = 2\int d\tau \widetilde{G}_{QP}(\tau) \circ \widetilde{G}^t_{QP}(-\tau) e^{i\omega_n \tau}$$

$$\widetilde{H}_{QP} = \widetilde{Z}^{1/2}\left(\widetilde{H}_H + \widetilde{\Sigma}(i\omega_n = 0)\right)\widetilde{Z}^{1/2}$$

$$\widetilde{Z} = \left(1 - \frac{\widetilde{\Sigma}(i\omega_n = 0)}{\partial(i\omega_n)}\right)^{-1}$$

$$\widetilde{W}^{-1}(i\omega_n) = \widetilde{V}^{-1} - \widetilde{\chi}(i\omega_n)$$

$$\widetilde{\Sigma}(i\omega_n) = -\int d\tau \widetilde{G}_{QP}(\tau) \circ \widetilde{W}(\tau) e^{i\omega_n \tau}$$

$$\simeq \widetilde{\Sigma}(i\omega_n = 0) + i\omega_n \frac{\widetilde{\Sigma}(i\omega_n = 0)}{\partial(i\omega_n)}$$

[1] A. Kutepov, K. Haule, S. Y. Savrasov, and G. Kotliar, Phys. Rev. B 85, 155129 (2012).
[2] A. Kutepov, S. Y. Savrasov, and G. Kotliar, Phys. Rev. B 80, 041103 (2009).

Self-consistent DMFT from QPGW

$$\widetilde{G}_{QP}(\mathbf{k}, i\omega_n) = (i\omega_n + \mu - \widetilde{H}_{QP}(\mathbf{k}))^{-1}$$

$\widetilde{P}(\mathbf{k})$ Using MLWF, U and J from cRPA

$$G_{loc}(i\omega_n) = \frac{1}{N_k} \sum_{\mathbf{k}} \widetilde{P}(\mathbf{k}) \left\{ \widetilde{G}^{-1}_{QP}(\mathbf{k}, i\omega_n) - \widetilde{P}^{\dagger}(\mathbf{k}) \left(\widetilde{\Sigma}_{imp}(s, i\omega_n) - \widetilde{\Sigma}_{DC}(i\omega_n) \right) \widetilde{P}(\mathbf{k}) \right\}^{-1} \widetilde{P}^{\dagger}(\mathbf{k})$$

$\Sigma_{imp}(i\omega_n)$ From CTQMC impurity solver

[1] P. Werner, et.al., Phys. Rev. Lett. 97, 076405 (2006).
[2] K. Haule, Phys. Rev. B 75, 155113 (2007).